The Effect of Heat Treatment and Cold-work on Precipitation and Recrystallization of BioDur108 High Nitrogen Austenitic Stainless Steel

F. Ghaderi *[1] , SH. Kheirandish [2]

Iran University of Science and Technology, School of Material Science and Engineering, Tehran, Iran

Abstract

HNS (High Nitrogen Austenitic Stainless Steel) steel is an attractive material due to its unique combination of outstanding mechanical and corrosion resistance properties in the medical and industrial applications. Despite the excellent traits, brittle precipitates (during ageing) could subvert the structure. Many studies were performed on the ageing reactions and the deposit nature. In this paper the effect of heat treatment and cold-work on precipitation and recrystallization behaviour in the sensitive deposition zone of BioDur108 HNS steel was investigated. For this purpose, Samples of high nitrogen austenitic stainless steel with cold-work values of 0, 40, and 60% were subjected to isothermal annealing at 4 temperatures of 850, 900, and 950, and 1000 ° C, for a constant time of 30 minutes, followed by water quenching. Microstructural characterization was carried out via optical microscopy and EDS tests. Vickers Hardness test was performed. In all cold-worked samples, recrystallization occurred before deposition. The sensitive deposition temperature was decreased with the cold-work percentage. Sensitive deposition temperatures were 950, 900 and 850°C for 0, 40, and 60% amount of cold-work, respectively. No carbide was formed and the precipitates were the predominant Cr_2N and a little Sigma phase. The primary reason, causing the hardness growth, was the Cr_2N deposition.

Keywords: BioDur 108, HNS Steel, Sensitive deposition temperatures, Solution annealing, Cold- work, Cr_2N.

1. Introduction

HNS steels were developed as early as 1941. In recent times the interest in such steels has been renewed because of the improvement in the level of mechanical properties and corrosion resistance by replacing carbon with nitrogen in conventional steels. Moreover, Nitrogen has greater solid-solubility than carbon, is a strong austenite stabilizer and a potent interstitial solid-solution strengthener. For these reasons nitrogen addition to steel has been extensively studied in the last 40 years [1-7].

**Corresponding author*
Email:ghaderi.fateme2013@gmail.com
Address: Iran University of Science and Technology(IUST), School of Material Science and Engineering, Tehran, Iran
1.B.S.
2.Professor

HNS steel is especially used in medical applications such as; implantable orthopaedic devices, high-strength surgical instruments, hypoallergenic jewellery; due to the nonmagnetic property that eliminates the allergenic demerits of the expensive nickel, including swelling and skin allergies. Despite these profits, high nitrogen content will induce brittle precipitates during the ageing treatment, hot forming or welding process [8].

Hua-Bing Li investigated the solution-treated (ST) condition and ageing precipitation behaviour of 18Cr-16Mn-2Mo-1. 1N high nitrogen austenitic stainless steel (HNS). In his study, hexagonal intergranular and cellular Cr_2N precipitates were gradually increased in the isothermal ageing treatment. Cr_2N caused the decrease in the impact toughness and led to the brittle intergranular fracture. The ultimate tensile strength (UTS), yield strength (YS) and elongation (El) were deteriorated [9].

Zhou-Hua Jiang investigated the microstructural evo-

lution of 18Cr18Mn2Mo0.77N in the ageing treatment. In his study, intergranular and cellular Cr_2N precipitated gradually in the isothermal ageing treatment. Cr_2N and the intermetallic χ phase caused the impact toughness a monotonic decrease and led to the brittle intergranular fracture. The tensile strength and elongation deteriorated obviously[10].

Several other authors [11, 12] have studied the ageing response in HNS steel and its relationship with physical and mechanical properties, but this concept needs further precise systematic investigations [8]. This project investigates the sensitive deposition zone of BioDur108 and the effect of solution annealing and cold-work on the precipitation and recrystallization trend in the parallel and crosswise. The results of this study are to increase the service life of production parts and reduce supply costs.

2. Experimental Details

Biodur108 samples, after hot rolling at 1200 ° C, were annealed at 1100 ° C and subjected to 0, 40, and 60% amount of cold-work. The chemical composition of the steel is stated in table 1. The annealing conditions were selected based on the temperature and time conditions, mentioned in the researches on the austenitic stainless steel [7]. Samples were annealed at 850, 900, 950, and 1000 ° C, a constant time of 30 minutes, in a resistance furnace with a volume of 2 litres and were followed by water quenching. Chemical etching was used for microstructural studies. The etching solution was glycerol at room temperature, which contained 3 parts glycerin, 2 to 5 parts hydrogen chloride and 1-part nitric acid. Microscopic images were taken with a Union Versamet3 light microscope. The linear density diagram and sediment surface graph were plotted by ImageJ. Vickers hardness test was performed, using ESE-Way 5592 with a force of 30 kg by ASTM-E18 standard[13] with a diamond penetrator in the shape of a square pyramid of al-Qaeda and the experiment was repeated 3 times for each sample on average. Precipitate type determination was carried out by EDS results.

3. Result and Discussions

3.1. Heat Treatment

Figure 1 shows light microscope images of the samples with 0% amount of cold-work, annealed at a)850 ºC, b)900 ºC , and c)950° C, a constant time of 30 minutes; the sediment Linear Density of each sample is plotted on the right. As shown the sediment linear density (LD) diagram traced the deposition intensity at 950° C (Fig. 1-c).

Table 1.Biodur108 chemical composition in terms of weight percentage of element.

Element	N	O	H	Al	P	S	Cu	Si	Mo	Mn	Cr	C
Weight percentage	1.1	.0047	.00003	.04	.003	.003	.32	1.41	1.50	22.1	19.8	.04

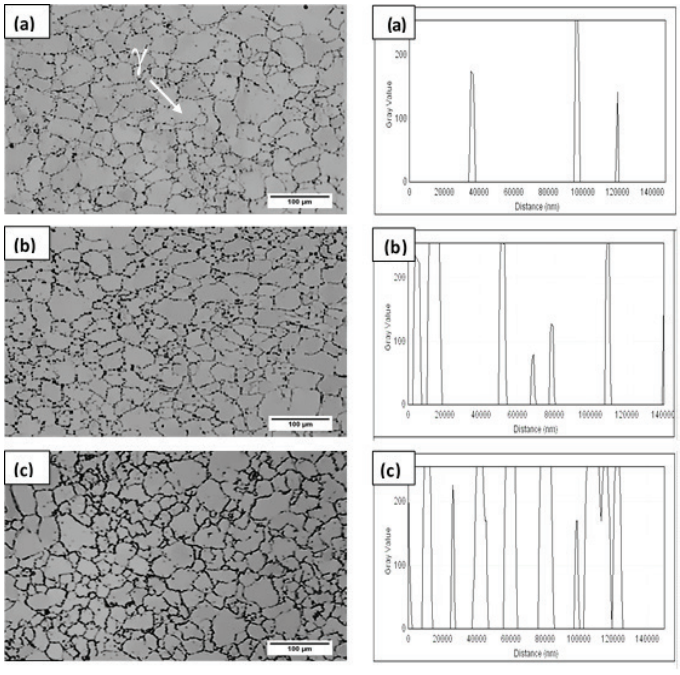

Fig. 1. On the left: optical microscope images of the samples with 0% amount of cold-work solution annealed at temperatures of a) 850 ° C, b) 900 ° C and, c) 950 ° C, each for 30 minutes; on the right: sediment Linear Density(LD) diagram of each sample.

Due to Figure 1, only the austenite phase (shown by white arrow) and precipitates were detected. Equations 1 and 2 were used for calculating Ni_{eq} and Cr_{eq}; thus finding the microstructure based on the cheflear diagram (Fig. 2) [2]. Equation 3 determines the minimum amount of nitrogen, required for the total austenite microstructure. In this article, the calculated Ni_{eq} and Cr_{eq} were, 40 , and 25 respectively, which based on the cheflear diagram, results in the total austenite matrix; Furthermore, [%N] min (equation3) is 0.5, which compared to 1.1 (in the present study) confirms the result (no possible ferrite formation).

$$Ni_{eq} = Ni + Co + 0/5Mn + 0/3Cu + 25N + 30C \quad \text{Eq. (1)}$$

$$Cr_{eq} = Cr + 2Si + 1/5Mo + 0/5V + 5/5Al + 1/75Ti + 0/75W \quad \text{Eq. (2)}$$

$$[\%N]\ min = -0/88(wt\%C) + 0/046(wt\%Cr) - 0/0009(wt\%Mn) + 0/038(wt\%Mo) - 0/053(wt\%Si) + 0/082(wt\%Ni) - 0/208(wt\%Cu) - 0/032(wt\%W) - 0/278 \quad \text{Eq. (3)}$$

Figure 3 shows Light microscope images of the samples with 40% amount of cold-work, annealed at a) 850 ºC, b)900 ºC , and c)950 ° C for 30 minutes; the sediment Linear Density is plotted on the right. As shown the deposition gravity is traced at 900°C by LD diagram (Fig. 3-b). The coaxial grains (shown by white arrow) are specified. The behaviour of recrystallization and deposition of a deformed alloy in austenitic stainless steel, during solution annealing, follows Equations 4 and 5 [12]. Consequently, if the supersaturated solid solution is deformed and annealed, equations 4 and 5 will affect each other until the recrystallization progress [12, 14]. Thus and considering the coaxial grains in Figure 3, recrystallization has been occurred before deposition.

$$t_P = K_P \exp\left(\frac{\Delta G^* + Q_D}{RT}\right) \quad \text{Eq. (4)}$$

$$t_R = K_R \exp\left(\frac{Q_R}{RT}\right) \quad \text{Eq. (5)}$$

t_p and t_R are the precipitation time during annealing and the recrystallization time, respectively (Equations 4 and 5). K_p and k_R are constants, Q_D and Q_R, the penetration and recrystallization activation energy, respectively, and ΔG *, the critical germination work [14]. During the annealing of cold-worked samples, precipitates, formed in dislocations, sub-boundaries and inside sub-grains, cause them to lock, restraint their moving, rearranging and recovery to a certain extent. They prevent the growth of sub-grains, their migration, and ultimately avoid the formation of recrystallization buds during polygonization. The said matters are represented in the form of Equation 6 [11, 14].

$$P = P_D - P_Z = \frac{\alpha Y_S}{R} - 3f_v\frac{Y_b}{2r} \quad \text{Eq. (6)}$$

In Equation 6, P is the sub-grain growth driving force, P_D, the intergranular joint energy, P_Z, the Zener pressure due to the grain boundary locking by second phase particles, R, and r, the Sub-grain radius and second the phase particle radius, respectively, fv, the second phase particle volume fraction, Y_S, the general phase energy of sub-grain boundary, and Y_b, the typical phase energy affecting the lock of second phase particles. The initial cold-work increases the locking pressure or Zener pressure by intensifying deposition (Equation 3). This reduces the driving force of sub-grain growth (P), therefore reducing the recrystallization driving force [14]. As a result, in Figure 3, the reason for the recrystallization cessation could be due to the severe deposition at grain boundaries and within the grains.

Figure 4, shows light microscope images of the samples with 60% amount of cold-work, annealed at temperatures of a)850 ºC, b)900 ºC, c)950 °C, a constant time of 30 minutes; and on the left, the linear density of each sample. As shown: The deposition gravity is traced at 850 ° C by the LD diagram (Fig. 4-a), but still, a small number of elongated grains (during cold-work) are existed (area shown by arrow). Thus, and due to the equations 1 and 2, the recrystallization occurred before the onset of deposition and was not completed [12, 14].

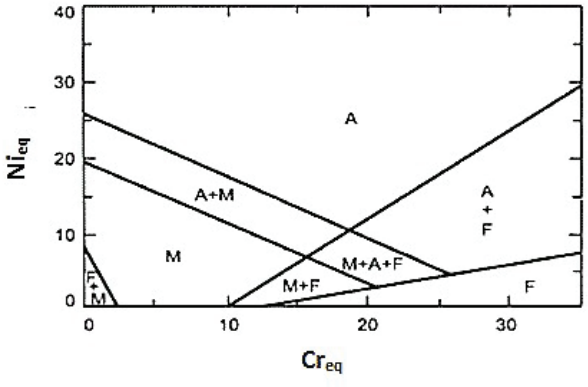

Fig. 2. Cheflear diagram[2].

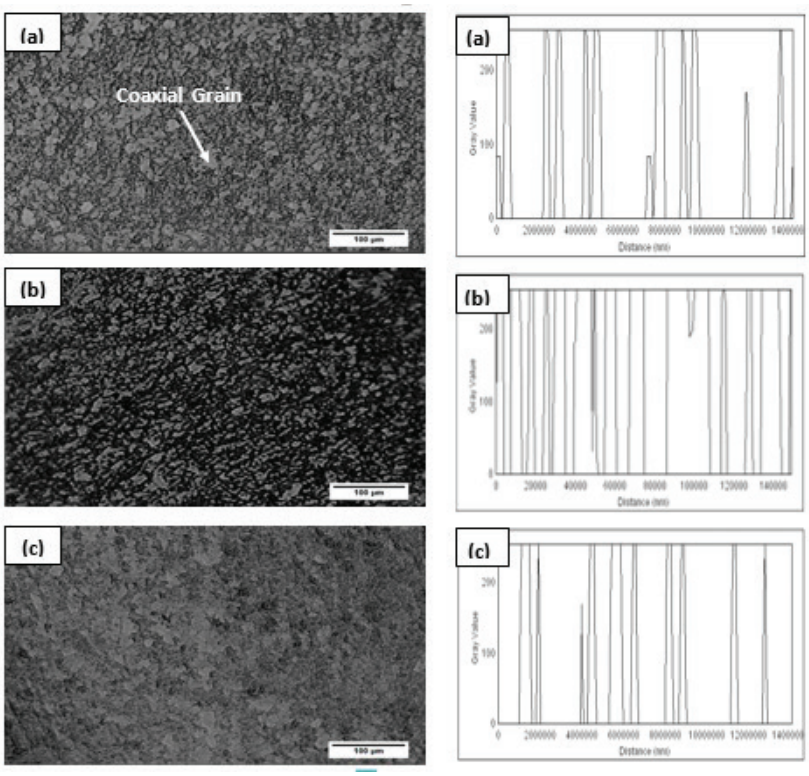

Fig. 3. On the left: optical microscope images of the samples with 40% amount of cold work, solution annealed at the temperatures of a) 850 ° C, b) 900 ° C and, c) 950 ° C, each for 30 minutes; on the right: sediment Linear Density(LD) diagram of each sample.

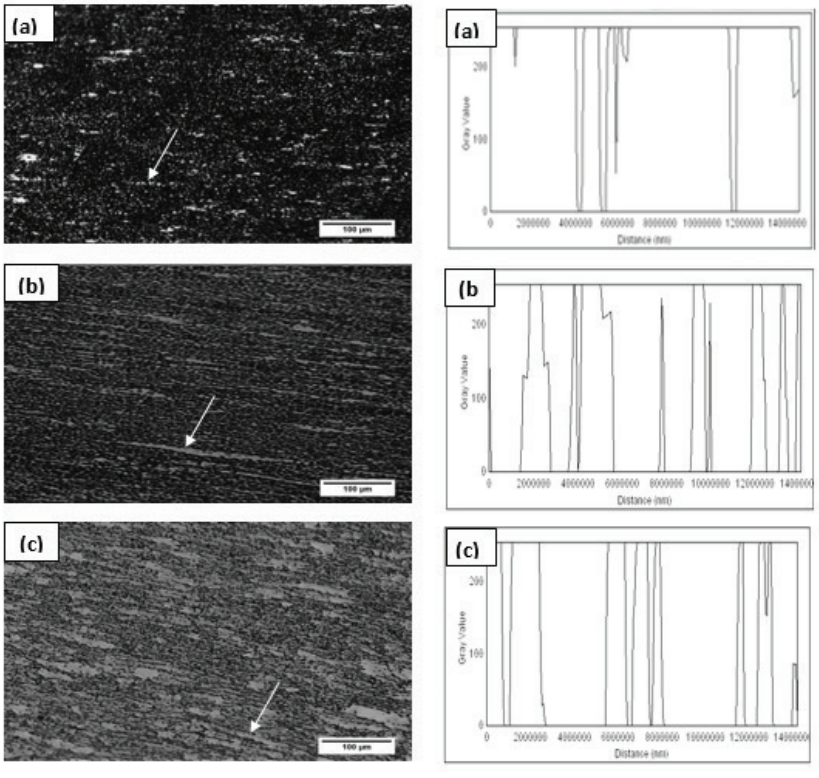

Fig.4. On the left: optical microscope images of the samples with 60% amount of cold-work, solution annealed at the temperatures of a) 850 ° C, b) 900 ° C and, c) 950 ° C, each for 30 minutes; on the right: sediment Linear Density(LD) diagram of each sample.

Figure 5 stands for the sediment surface plot of the samples with 0% amount of cold-work, annealed respectively at a) 850 ºC, b) 900ºC , and c)950ºC; samples with 40% amount of cold-work, annealed respectively at d)850 ºC, e)900 ºC , and f)950 ºC; , and samples with 60% amount of cold-work, annealed respectively at g)850 ºC, h)900 ºC , and i)950 ºC; all samples were annealed at each temperature a constant time of 30 minutes. Due to Figure 5, the maximum sediment volume fraction for different amount of cold-work obtained at the sensitive deposition temperature, which was 950 ºC (Figure 5-c), 900 ºC (Figure 5-e), and 850 ° C (Figure 5-g), for 0%, 40%, and 60% amount of cold-work, respectively.

3.2. Precipitate Type Characterization

The precipitate type specification was carried out by EDS test (results are given in table 2 and Figures 6), Choosing two points of precipitate phase in the sample with 60% amount of cold-work, annealed at 850 ° C, 950 ° C , and 1000 ° C, for 30 minutes. From EDS results at 850 ° C (a) and 950 ° C (c), nitrogen and high amounts of chromium, manganese and iron were specified, identifying the chemical composition of Cr_2N, equal to $(Cr_{0/73}Fe_{0/17}Mn_{0/10})_2N$, which indicated the formation of this phase. Results of other points in Table 2 corresponded to the chemical composition of Sigma phase) σ (, (Fe_5Cr_{33} Mn_{17}), which contained 0 wt. % of nitrogen and high amounts of manganese, chromium, and iron. Due to the chemical composition of the phases; Chi (X) ($Fe_{36}Cr_{12}Mo_{10}$), and Laveh (η) (Fe_2Mo), indicating the principal constituent, molybdenum, rarely existed in the analysis, they weren't formed. Scientists' researches on the austenitic stainless steel [12-15], confirmed the Cr_2N and Sigma phase deposition.

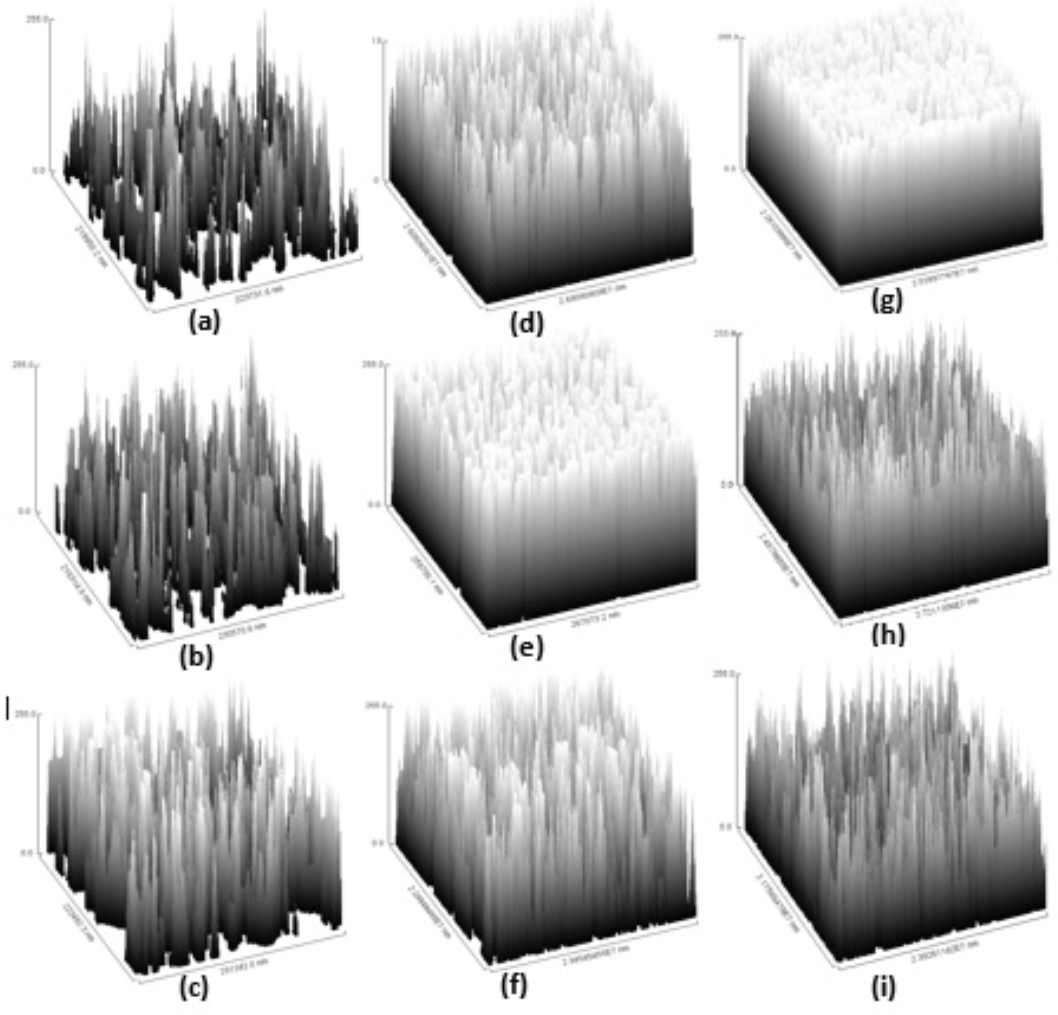

Fig. 5. Sediment surface plot of the samples with 0% amount of cold-work, annealed respectively at a) 850, b) 900 and, c)950ºC; samples with 40% amount of cold-work, annealed respectively at d)850, e)900 and, f)950 ºC; and, samples with 60% amount of cold-work, annealed respectively at g)850, h)900 and, i)950 ºC; all samples were annealed at each temperature a constant time of 30 minutes.

Table 2. EDS results of the sample with 60% amount of cold-work, annealed at 850°C, 900°C, 950°C and 1000 °C, a constant time of 30 minutes.

Element/Temperature	Fe (Wt. %)	MN (Wt. %)	Cr (Wt. %)	N (Wt. %)
850°C(a)	43.42	19.41	22.22	3.87
850°C(b)	44.1	19.58	18.59	0
950°C(c)	39.62	16.60	20.68	3.59
950°C(d)	36.95	18.92	16.95	0
1000°C(e)	46.46	23.13	23.41	0
1000°C(f)	52.92	23.47	23.61	0

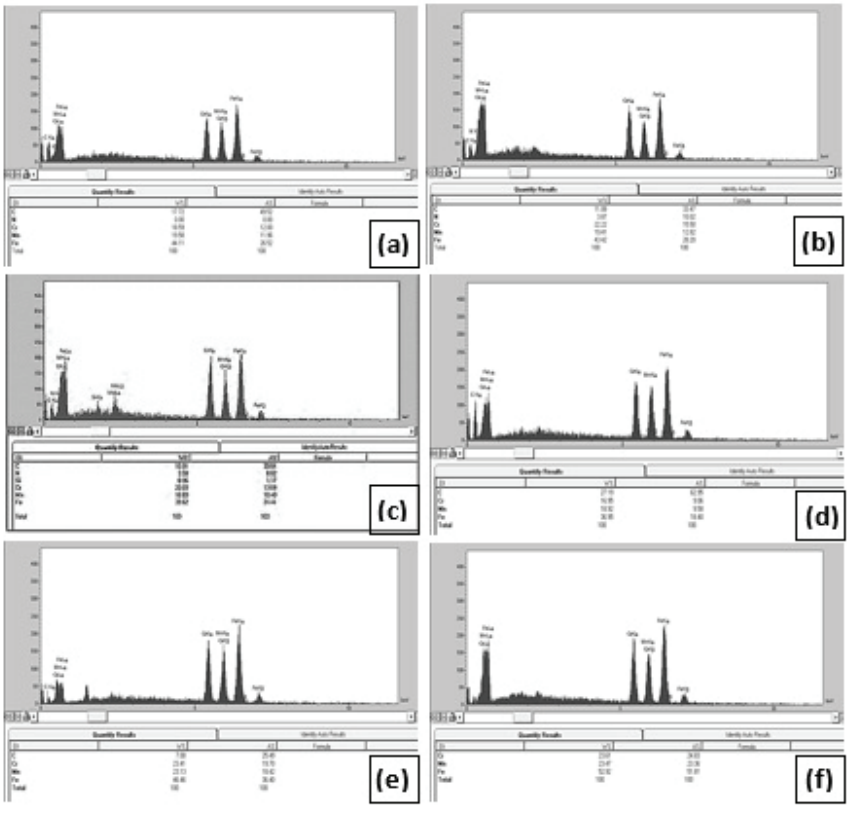

Fig. 6. EDS analysis, from two sediment points of the annealed sample with 60% amount of cold-work at: a, b)850°C, c, d)950°C and, e, f)1000°C, respectively.

According to Table 2, nitrogen was not detected at 1000 ° C. The cause is attributed to the dissolution of a significant amount of Cr_2N sediments [7]. Due to the nitrogen depletion near Cr_2N, σ-phase deposited (because of no nitrogen solubility [8]. To scientist researches [7-10], after annealing the cold-worked samples at 850 ° C, the predominant sediment was Cr_2N with a small amount of sigma phase within the grains. Cr_2N appeared in the form of discontinuous cellular sediments at the grain boundaries. The initial cold-work before solution annealing accelerated and increased the process of sigma phase deposition[15]. Therefore, and due to table 2 and other researches [7, 15], the precipitates in the sample with 60% amount of cold-work under 30 minutes of annealing at 850 ° C, were mainly Cr_2N and a little sigma phase. Figure7 shows the temperature-time (T-T) diagram of

Cr_2N deposition in CrNiN and CrMn austenitic stainless steel [7].

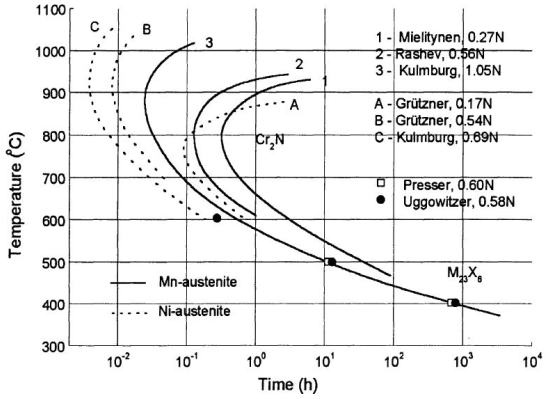

Fig. 7. T.T Diagram; deposition behaviour in CrNiN and CrMnN austenitic steels [7].

By Figure 7, Line 3 corresponds to the manganese austenitic steel with 1.05 wt. % nitrogen. The time required for Cr_2N deposition was approximately 2.5 minutes at 850 ° C, 3 minutes at 950 ° C ,and 5 minutes at 1000 ° C [7]. consequently, in the present study (very close to that of manganese austenitic stainless steel; line 3, Figure 7), and considering the 30-minutes of annealing at 850 ° C, 950 ° C , and 1000 ° C, Cr_2N deposited and was the predominant sediment.

Research performed on Cr18Mn12N0/48 high nitrogen austenitic steel [14], confirmed the formation of Cr_2N and Sigma phase in the cold-worked samples. The principle precipitate, after annealing for 1 hour, was Cr_2N and sigma phase dissolved inside the grains.

Nitrogen high weight percentage resulted in the small amount of sigma phase, the austenite stability enhancement (as a result of nitrogen uniform distribution), the lack of intermetallic phases (because of no nitrogen solubility) , and the chromium activity reduction in the austenite. In addition, the crystal structure of sigma phase was incompatible with the ground (austenite), and asymmetric germination required the high-energy joint cycle, provided with the high amount of driving force. The initial cold-work before solution annealing operation accelerated and increased the sigma phase deposition process[7]. Cold-work increases the distortion energy and misalignment locking; consequently, the sigma phase usually forms at the grain boundaries; as well as inside the grains. The microstructural defects, such as slip bands and mechanical twinning at higher cold-works are also considered [15].

In the sample with a 0% amount of cold-work, the sigma phase wasn't formed; because of the high nitrogen percentage and the little driving force [7]. In addition, nitrogen works better than carbon in eliminating the brittle sigma phase. The great amount of nitrogen in HNS steel reduces the ferrite (δ), thus delaying the conversion to the sigma phase [16-18]. By Figure 8, the discontinuous cellular sediments at the grain boundaries (shown by white arrow) confirm the Cr_2N deposition [15].

By Figure 7, the time required for the $M_{23}C_6$ carbide deposition in the steel containing 0.27 wt. % of nitrogen, was close to one hour at 850 ° C, which was increased at higher temperatures [7]. Nitrogen delays the deposition of $M_{23}C_6$ carbides (Figure7) and at temperatures above 600 ° C, is replaced by Cr_2N. This is because of the chromium penetration rate increase by nitrogen, no nitrogen solubility in carbides , and the higher nitrogen diffusion coefficient than carbon [7, 18]. Considering the weight percentage of nitrogen in the present study (1.1 wt. %), the $M_{23}C_6$ carbide formation time at 850 ° C was more than one hour and could increase at higher temperatures (up to 1000 ° C). Therefore, in all the samples, $M_{23}C_6$, M_6C (Since the origin of M_6C carbide is $M_{23}C_6$ and MC weren't formed[7]. The absence of Titanium, niobium, and nickel (about 0.05%) in the present study, led to the lackof MC[7]. In a conclusion, no carbide was formed.

3.3. Mechanical Properties

Tables 3, 4 and 5 stands for the hardness versus temperature for 0, 40 , and 60% amount of cold-work, respectively.

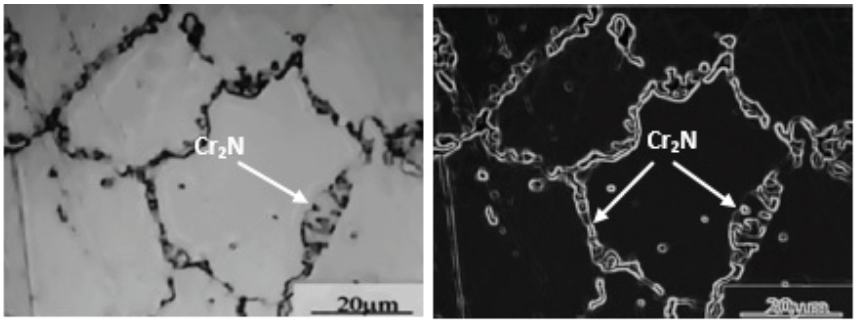

Fig. 8. On the left, OM image of the sample with 0% amount of cold-work, solution annealed at 900° C for 30 minutes; on the right, sediment edge, processed by ImageJ.

Table 3. Hardness versus temperature for the sample with 0% amount of cold-work.

Temperature(ºC)	25	850	900	950	1000
Hardness(HV)	332	357	374	380	357

Table 4. Hardness versus temperature for the sample with 40% amount of cold-work.

Temperature(ºC)	25	850	900	950	1000
Hardness(HV)	541	381	436	387	370

Table 5. Hardness versus temperature for the sample with 60% amount of cold-work.

Temperature(ºC)	25	850	900	950	1000
Hardness(HV)	552	598	527	496	467

By Figure 9, standing for the hardness diagram versus temperature for; a) 0%, b) 40% , and c) 60% amount of cold- work; and the sediment volume fraction diagram versus temperature for; d) 0%, e) 40% , and f) 60% amount of cold- work:

1- According to researchers [19, 20], the hardness increase with the amount of cold-work in the ambient temperature is attributed to the high amount of sediments, their smaller size, their more uniform distribution within the grains , and the sediment germination facilitation by stacking faults and twins. The increase in the volume percentage of defects, especially the dislocation density and slip bands (during the cold-work), are also considered. By the research on Cr18Mn12N0/48 high-nitrogen austenitic stainless steel [15], cold-work increases the deposition rate due to the dislocation length reduction and the density augmentation. Moreover, a large number of defects in the crystal lattice, around the grain boundaries and the misplaced channels, accelerate the penetration. From these thermodynamic vesicles, in cold-worked samples (in the present study), sediment germination energy reduction accelerated the deposition. To researchers [19,20], the sediment formation in the form of fine particles, (less than 1 μm) scattered inside the grains, increased the hardness and the strength. The hardness correlation with the size of sediment cells follows the Hall-Patch Equation (Eq. 7).

$$H_V = H_{OV} + K_H.d^{1/2} \qquad \text{Eq. (7)}$$

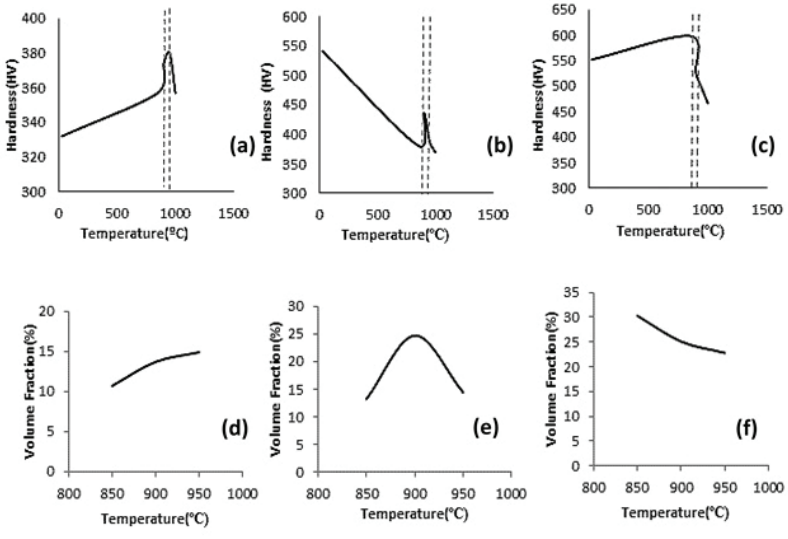

Fig. 9. Hardness diagram versus temperature for a) 0%, b) 40% and, c) 60% amount of cold-work; and the sediment volume fraction diagram versus temperature for d) 0%, e) 40% and, f) 60% amount of cold-work.

In Equation 7, H_{OV} and K_H are constants, d, the sediment cell diameter , and $H_{V,}$ the Vickers hardness. 2-Severe deposition at lower temperatures prevented the hardness decrease (due to the recrystallization), which was disappeared by the temperature rising [14, 21]. In all cold-worked samples at 1000 ° C, hardness decreased, attributed to the dissolution of sediments and the removal of Zener pressure [8, 15].

By Figure 9, the hardness peak coincides with the sensitive deposition temperature, which [17- 21] confirms the Cr_2N precipitation as the main reason for the hardness growth in cold-work samples. The light precipitation deduced the low hardness amount at 850 ° C (Figure 9; a and d).

Due to Figures 3 and 9 (b and e), recrystallization occurred before precipitation. Since the minimum amount of sediments was at 850 ° C, the reduction in the hardness from ambient temperature to 850 ° C, considered as a result of recrystallization and the matrix Nitrogen depletion (due to the nitrogen long-term diffusion to form Cr_2N sediments). At 900° C and 950 ° C, only the sedimentation was effective on the hardness (because of the recrystallization consistency). Considering scientists' results [17- 22] and the coincidence of the hardness peak with the sensitive deposition temperature, the cause of the hardness increases up to 900 ° C was due to the Cr_2N propagation and Sigma sediments, which
principally was attributed to the Cr_2N dominant deposits.

By Figure 4 and 9(c and f):

Recrystallization occurred before sedimentation. The hardness increases up to 850 ° C, ascribed to the deposition intensity, preventing the manifestation of the hardness decrease (due to the recrystallization). Considering the coincidence of the hardness peak with the sensitive deposition temperature (850° C), the hardness growth was mainly attributed to the Cr_2N deposits and nominally to Sigma sediments [17-22].

4. Conclusions

- In the cold-work samples, annealed for 30 minutes at 850° C, 900° C, 950° C , and 1000 ° C, no carbide was formed and the principal precipitate was Cr_2N (with a little sigma phase). In the sample with 0% amount of cold-work, only Cr_2N was deposited.
- Sensitive deposition temperatures were 950,900, 850 ° C, respectively for the samples with 0%, 40% , and 60% amount of cold-work.
- In all cold-worked samples, recrystallization occurred before deposition.
- The reason for the hardness increase was the formation of Cr_2N deposits.

Nomenclature

ΔG^*	Critical germination work
a	Constant
d	The diameter of the sediment cell
f_V	The volume fraction of the second phase particles
H_{ON}	Constant
H_V	Vickers hardness
K_H	Constant
K_p	Constant
K_R	Constant
P	Driving force for the growth of the sub-grains
P_D	Driving force due to the energy of the intergranular joint
Pz	Zener pressure
Q_D	Penetration activation energy
Q_R	Recrystallization activation energy
R	Sub-grain radius
r	Radius of the second phase particle
T	Temperature
t_p	Time of precipitation during annealing
t_R	Recrystallization time
Y	The energy of the interface
Y_b	Typical phase energy affecting the locking of the second phase particles
Ys	Common phase energy of the sub-grain boundary

Reference

[1] M. Salehi, SH. Kheirandish, M. Abbasi: The Effects of Cold-work on the Microstructure and Mechanical Properties of 108biodur Austenitic Stainless Steels, IUST, Tehran, (2015), 41. (In Persian)

[2] M. Salehi, SH. Kheirandish, M. Abbasi: Metall. Mater. Eng., 29 (2018), 55.

[3] H. Chandra, P. J. Uggowitzer: Scripta Metallurgica., 21 (1987), 513.

[4] P. Marshal: Austenitic Stainless Steels, Microstructure and Mechanical Properties, Elsevier sci., Springer Netherlands (1984) 58.

[5] J. Sieslak, A. M. Ritter, V. F. Savage: Weld. J., 10(1984), 133.

[6] N. Sutala: Metall. Mater. Trans. A. Phys. Metall. Mater. Sci., 13 (1982), 2121.

[7] G. Gavriljuk, H. Berns: Springer Sci., Verlag Berlin Heidelberg, (1999), 51.

[8] T. H. Lee, C. S. Oh, C. Gillee, S. J. Kim, S. Takaki: Scripta Materialia, 50 (2004), 1325.

[9] H. Bing, Z. Jiang, H. Feng, D. P. Zhan: J. Iron Steel Res. Int., 19 (2012), 43.

[10] A. Etemad, G. Dini, S. Schwarz, Materials Science and Engineering: A, 742(2019), 27.

[11] F. J. Humphreys, , M. Hatherly: Recrystallization and Related Annealing Phenomena, Elsevier Ltd, U. K(2004), (2004), 50.

[12] S. Feng, L. Xiao-wu, Q. Yang, L. Chun-ming: Ageing Precipitation and Recrystallization Behaviour after Cold Compression by 10% in High-Nitrogen Austenitic Stainless Steel, PRICM 8, (2013), 571.

[13] ASTM standards (2014), ASTM-E18 standard, https://www.astm.org/Standards/E18.htm

[14] S. Feng, L. J. Wang, W. F. Cui, C. M. Liu: Adv. Mat. Res, 20 (2007), 95.

[15] S. Feng , X. W. Li, Y. Qi, C. M. Liu: Key. Eng. Mater, 531-532 (2012), 97.

[16] F. Vanderschaeve, R. Taillard, J. Foct: J. Mater. Sci, 30 (1995), 6035.

[17] J. Y. Li, H. Liu, P. Huang: J. Cent. South Univ, 19 (2012), 1189.

[18] W. C. Hsieh, D. Y. Lin, W. Wu: Mater. Sci. Eng. A, 467 (2007), 181.

[19] N. C. Santhi Srinivas , V. V. Kutumbarao: Trans Indian Inst Met, 64(2011), 331.

[20] R. Reed-hill: Phisical Metallurgy Principles , IUST, Tehran, (2007). (In Persian)

[21] F. Ghaderi, SH. Kheirandish: The Effect of Heat Treatment and Cold-work on Precipitation and Recrystallization of BioDur 108 HNS Steel, IUST, Tehran, (2014). (In Persian)

[22] A. F. Padilha, P. R. Rios: ISIJ Int, 42(2002), 325.